Available online at www.sciencedirect.com
SCIENCE DIRECT
Journal of Molecular Catalysis A: Chemical 242 (2005) 81–90
JOURNAL OF MOLECULAR CATALYSIS A: CHEMICAL
www.elsevier.com/locate/molcata

Study of nickel catalysts supported on Al_2O_3, SiO_2 or Nb_2O_5 oxides

A. Jasik [a], R. Wojcieszak [b], S. Monteverdi [b], M. Ziolek [a], M.M. Bettahar [b,*]

[a] *Faculty of Chemistry, Adam Mickiewicz University, Grunwaldzka 6, 60-780 Poznan, Poland*
[b] *UMR 7565, Catalyse Hétérogène, Faculté de Sciences, Université Henri Poincaré, Nancy-I, BP 239, 54506 Vandoeuvre les Nancy Cedex, France*

Received 13 June 2005; received in revised form 14 June 2005; accepted 7 July 2005
Available online 2 September 2005

Abstract

We have studied nickel classical catalysts supported on Al_2O_3, SiO_2 and Nb_2O_5 oxides, using simple (SIM) or EDTA-double impregnation (DIM) methods. Non-classical catalysts were obtained by pretreatment of the SIM or DIM nickel precursors in aqueous hydrazine at 353 K. The catalysts were characterized by H_2-adsorption, H_2-TPR, isopropanol decomposition and FTIR measurements. They have been tested in the gas phase hydrogenation of benzene. The results obtained show that the support surface acidity order was: $SiO_2 < Al_2O_3 < Nb_2O_5$. The catalysts exhibited various nickel species due to the existence of various metal–support interaction strengths. As a consequence, the reducibility, surface or hydrogenating properties changed as a function of the nature of the support or method of preparation. The best performances were obtained with the silica support which seemed to interact less with the nickel. The metal–support interactions are highest when niobium oxide is used as the matrix. Ni impregnated on niobia was not active at all, due to very strong metal–support interactions. The interaction of aqueous hydrazine with the catalyst in the reduction conditions was examined. It was shown that hydrazine formed stable complexes with nickel, whereas it adsorbed on the support with a strength depending on the nature of the oxide.

Keywords: Nickel; Catalyst; Support; Double impregnation; Benzene hydrogenation

1. Introduction

The activity and selectivity of a supported metal catalyst are strongly influenced by the amount of metal, the size of dispersed metal particles, the preparation method and the support composition [1–3]. To improve the catalyst activity and its durability, it is necessary to obtain a well-dispersed active phase in the catalyst [4]. Several methods can be applied to obtain highly dispersed metals on the support surface [5]. Supported metal catalysts are commonly prepared by metal salt impregnation. If the support is microporous, it will imbibe a solution of a metal salt; drying, calcination (optional) and reduction will generate small metal particles. The classical method of the support impregnation results in obtaining small metal crystallites but only at very low metal contents in the catalyst [6]. It is also possible to obtain small metal crystallites by co-precipitation, but such catalysts are very difficult to reduce [7].

Supported nickel catalysts are most effectively prepared through the optional combination of high dispersion and metal loading. Small metal particles may be formed on the surface of the support to which they are more or less firmly anchored, and on which they are effectively separated from each other. The average distance between the particles will depend on the metal content, the particle size and the surface area of the support [8].

Nickel catalysts were prepared by the double impregnation method (DIM) [9,10]. Previous findings and literature data allow to conclude that this preparation method is suitable for producing well-dispersed nickel/alumina-supported catalysts [9–12]. In DIM, there are two stages, one by one. The first one is the impregnation of inorganic support by H_2Na_2EDTA solution and then (after drying) impregnation by solution containing active metal ions. In contrast to the classical simple impregnation method (SIM) [13], in DIM preparation procedure the carrier is preliminarily "activated" (modified) by

* Corresponding author.
E-mail address: Mohammed.Bettahar@lcah.uhp-nancy.fr (M.M. Bettahar).

1381-1169/$ – see front matter © 2005 Elsevier B.V. All rights reserved.
doi:10.1016/j.molcata.2005.07.013

EDTA introduced by impregnation and dried; the following preparation steps are the same as in SIM [14]. Modification of the support using impregnation by H_2Na_2EDTA has influence on the way of metal bonding, which is added in the next stage of preparation. It changes the concentration of metal in catalyst and decreases average nickel crystals size. Application of H_2Na_2EDTA on the stage of preparation favored high active phase dispersion.

Presence of the EDTA adsorbed on the support surface assures homogenous distribution of the metal ions. The effect of the presence of EDTA is particularly visible in the low and average concentrations of metal ions. As the concentration of metal is increasing in impregnation solution, participation of favorable interaction EDTA–ion is gradually decreasing, which is caused by accelerated adsorption in support pores and the increase of the interactions between metal ions and hydroxyl surface groups [15].

Conventional supported metal catalysts are prepared by in situ reduction of a metal salt. The catalytic activity of the metal particles is strongly influenced by their size and shape [1,2,16–19]. However, it is often difficult to control the morphology of the final material, notably for impregnated catalysts [16–23]. An alternative method to obtain supported catalysts with well-defined metal particles is the preparation of supported catalysts from metal colloids.

Metal nanoparticles research has recently become the focus of intense work due to their unusual properties compared to bulk metal. The reason for such avid research arises from the drastic increase of the surface to volume ratio to such an extent that the material properties are determined much more by the surface atoms than by the framework atoms, with the result that the physical and chemical properties of the particles differ considerably from those of bulk solids [3–8]. They hold promise for use as advanced materials for electronic, magnetic, optical and thermal properties [9,10] and have also been applied in heterogeneous catalysis [7,24–27]. The chemical route for the preparation of such materials is of particular interest since it allows a better control of the structure at the microscopic level [28–40]. The chemical methods have generally involved the reduction of the relevant metal salt in the presence of a stabilizer such as linear polymers [6,41–44], ligands [44,45], surfactants [40,46–48], tetraalkylammonium salts [49,50] or heterogeneous supports [51–53] which prevent the nanoparticles from agglomerating.

Recent works have pointed out the interest of working in aqueous medium as a practical solution for the future in homogeneous and heterogeneous catalysis [54]. This prompted us to undertake a study of nickel nanoparticles obtained by reduction of nickel salts in aqueous medium and stabilized on a silica support of low surface area. The surface properties of the obtained catalysts were tested in gas phase hydrogenation of benzene.

Hydrazine was used because recent studies showed that it is a good reducing agent in aqueous medium for noble and transition metals ions [53,63–65]. As to the silica support, it is known not to give rise to nickel mixed oxides and to allow a better approach of the particle size effect in the behavior of supported nickel catalysts. Moreover, generally speaking, nickel-supported catalysts have been concerned with high surface area supports and nickel loading higher than 5 wt%. Also, the use of silica of low surface area and low nickel loading in the preparation of nickel based catalysts was expected to give rise to an important contribution to the existing corpus of literature on Ni/SiO_2 systems [20]. We were also encouraged in this way because preliminary results showed that, in aqueous medium, the nickel reduction process was enhanced in the presence of low surface area silica, whereas silica of high surface area tended to inhibit it.

In spite of the high number of studies published in the past decades, an increasing attention is paid to the hydrogenation of aromatics because of the stringent environmental regulations governing their concentration in diesel fuels [55–58]. Benzene hydrogenation has been chosen as the model aromatic feedstock [59,60]. This reaction has also been used as model reaction in heterogeneous catalysis by metals where metal–support interactions are involved [58–62].

In this paper, we show how the different methods of preparation change the properties of metal containing catalysts supported on different oxides. We have been working on nickel catalysts supported on Al_2O_3, SiO_2 and Nb_2O_5 oxides. The catalysts were characterized by hydrogen chemisorption, H_2-TPR technique, isopropanol decomposition and FTIR measurements. They have been tested in benzene hydrogenation. The catalysts were prepared with 1% Ni loading, using nickel acetate as precursor. The supported precursors were prepared by simple or double impregnation methods. Classical catalysts were obtained by calcination in air at 773 K, then reduction under hydrogen flow at 773 K. Non-classical catalysts were obtained by reduction of the precursor in aqueous hydrazine at 353K, then treated under hydrogen flow at 673 K (2 h) for activation. The study was carried out with catalysts of 1% Ni content because stronger metal–support interactions were expected to occur than for catalysts with greater nickel contents [1,2,15].

2. Experimental

2.1. Preparation

2.1.1. Classical catalysts

$H_2Na_2EDTA{\cdot}2H_2O$, $Ni(CH_3COO)_2$, alumina, silica and hydrated niobium oxide were purchased from POCH (99.9%), Fluka (99.0%), ALFA Johnson Matthey Company (99.97%), Ventron (99.8%) and CBMM (99.97%), respectively. The supports were dried at 363 K for 1 h before the impregnation procedure.

For the SIM, the appropriate quantity of the support was poured over nickel acetate solution with the appropriate concentration. After 15 min of rotation under vacuum, the mixture was heated and evaporated for 1 h. The obtained solid was dried at 383 K for 1 h (temperature ramp 3 K min^{-1}) and

then calcined (temperature ramp 5 K min^{-1}) at 773 K for 4 h in an air flow of 150 cm^3 min^{-1}.

For the DIM, the appropriate quantity of the support was poured over a solution of H_2Na_2EDTA with the appropriate concentration and stirred for 15 min. After filtrating and drying at 383 K for 1 h (temperature ramp 3 K min^{-1}), the obtained solid was impregnated with $Ni(CH_3COO)_2$ and calcined as described above for the simple impregnation.

2.1.2. Non-classical catalysts

In the preparation of nickel catalysts by the reduction with hydrazine, the metal phase is expected to proceed according to the following reaction [26]:

$$Ni^{2+} + N_2H_4 + 2OH^- \rightarrow Ni^\circ + N_2 + 2H_2O + H_2 \quad (1)$$

The preparation was performed under argon atmosphere (flow rate = 100 cm^3 min^{-1}) in a three-necked reaction flask of 250 ml dipping in a water bath. The reaction flask was fitted with a reflux condenser and a thermocouple for the control of the reaction temperature and connected to a gas microchromatograph (Agilent G2890A) for the analysis of the gases evolved during the reduction process. A suspension of the supported nickel precursor was stirred for 20 min at room temperature. The reaction mixture was slowly heated from room temperature up to 353 K. Then, 5 ml of 24–26% aqueous hydrazine in excess (>99%, Fluka) was added. The pH of the solution was 10–12 and remained almost constant. The green color of the solids changed to blue, that of the $[Ni(N_2H_4)_n]^{2+}$ complex formed [27,72]. Unfortunately, no reduction of nickel occurred: the blue color of the solid was not changed to dark and no hydrogen or nitrogen was detected in the exit gas [see Eq. (1)].

In case of the 1% Ni/EDTA/SiO_2 catalyst, the treatment with aqueous hydrazine provided desorption of nickel complex from the support surface. After hydrazine injection, the reactant solution became blue while the support changed color from green to white. This phenomenon could be explained by low Ni/EDTA complex compound stability in high pH conditions. When hydrazine was introduced in the liquid media, the Ni–EDTA complex desorption was observed; also, a more or less significant part of active phase was out of catalyst. The blue color is ascribed to the formation of $[Ni(N_2H_4)]^{2+}$ complex [72].

2.2. Equipment

A Bruker FTIR Vector spectrometer was used to detect infrared spectra of the samples. One milligram of sample was dispersed in KBr pellet with slight grinding for FTIR measurements at room temperature.

Chemisorption and thermal treatments experiments were carried out in a pulse chromatographic microreactor equipped with the catharometric detector of a microchromatograph (AT M200, Hewlett Packard) fitted with molecular sieve columns and MTI software.

Isopropanol decomposition was performed using a pulse microreactor and a helium flow of 40 cm^3 min^{-1}. The catalyst bed (0.05 g) was first activated at 673 K for 2 h under helium flow. The isopropanol conversion was studied at 523 K using 5 μl pulses of isopropanol. The gases were analyzed by CHROM-5 GC (2 m column with Carbowax 400 (80–100 mesh) at 338 K in helium flow) on line with microreactor and detected by TCD.

The gas phase hydrogenation reaction was carried out in a fixed bed quartz reactor. The reactant and product analyses were conducted on line in a Hewlett Packard 5730A FID gas chromatograph. Benzene, cyclohexane, cyclohexene and methylcyclopentane were analyzed with TCEP (2 m, 1/8 in.) and Sterling (3 m, 1/8 in.) columns, respectively. A Kontron software was utilized for data processing.

2.2.1. Chemisorption and thermal treatments

The chemisorption or thermal treatment was carried out over 0.1 g samples. The gases were purchased from Air Liquide. Oxygen traces were eliminated from argon (99.995%) and hydrogen (99.995%) by using a manganese oxytrap (Engelhardt), whereas helium (99.999%), air and oxygen diluted in argon were used as received.

The H_2-TPR study was carried out using H_2/Ar (1000 ppm H_2) mixture as a reductant (flow rate = 90 cm^3 min^{-1}). The sample was first flowed with argon at room temperature for 1 h, then heated at a rate of 5 K min^{-1} to 1123 K under the reductant mixture. Hydrogen consumption was measured with a thermal conductivity detector in Agilent G2890A series Micro GCs gas chromatograph operated at 333 K.

The degree of reduction was determined according to reference [66]. For all the catalysts, the sample was heated at rate of 10 K min^{-1} to 673 K for 2 h reduced in a flow of hydrogen pure (flow rate = 50 cm^3 min^{-1}). After the reduction, the sample was treated in a flow of argon at the reduction temperature for 1 h with a flow rate of 100 cm^3 min^{-1}. It was again purged at 723 K for 1 h. The oxygen adsorption was carried out using a mixture of O_2/Ar (100 ppm O_2) which was injected to the reactor at the same temperature with a flow rate of 100 cm^3 min^{-1}.

For the H_2-adsorption study, all the catalysts were previously reduced, then purged as described above. The reduced sample was cooled to room temperature under argon atmosphere and the reactant gas (100 ppm H_2/argon) was injected to the reactor ever 2 min.

Assuming spherical metal particles, the metal mean size was calculated from the following relation [67]: $d = 971/D$, where D is the metal dispersion as determined by H_2-adsorption.

2.3. Catalyst testing

The hydrogenation of benzene was carried out in a fixed bed quartz reactor. The catalytic experiments were carried out over 0.1 g of catalyst under a total flow of 50 cm^3 min^{-1}

under atmospheric pressure and in the temperature range 348–498 K.

Each reaction temperature was maintained constant until the steady state was reached, as indicated by gas chromatography analysis of the exit gases. The reactant feed gas was obtained by flowing H_2 in benzene (Merck, 99.5%) placed in a saturator maintained at 278.4 K in order to obtain a mixture of 1% benzene diluted in hydrogen.

3. Results and discussion

3.1. Characterization of the catalysts

The acidity of the supports used in this work was estimated on the basis of isopropanol dehydration. Intramolecular dehydration towards propene as well as intermolecular reaction producing diisopropyl ether occurs with the participation of acidic centers on the catalyst surface. For all matrices tested, propene was the main reaction product indicating acidity of the materials. However, the conversion of alcohol (indicating acidity) depended on the nature of the support (Fig. 1) in the following order: $SiO_2 < Al_2O_3 < Nb_2O_5$.

Because acidity of the supports is different, one can expect various strength of their interaction with nickel salt. In fact, the matrix exhibiting the highest acidity (hydrated Nb_2O_5) chemically reacted with Ni-acetate during the impregnation and calcination, as evidenced from IR spectra shown in Fig. 2. In case of both impregnated methods, the final materials exhibit well-resolved bands in the 500–1000 cm^{-1} region not characteristic for the initial support. It suggests the chemical reaction between nickel species and niobia support. The Ni/Nb_2O_5 system is known to give rise to strong metal–support interaction [68–72].

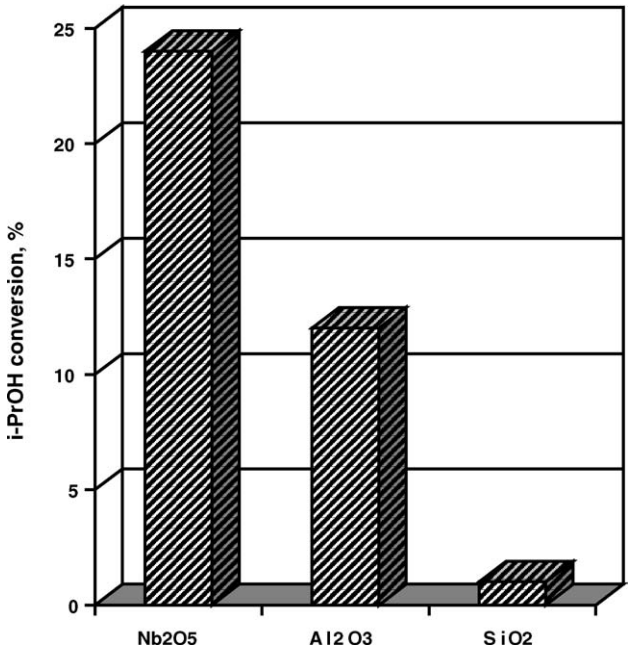

Fig. 1. Isopropanol decomposition at 523 K.

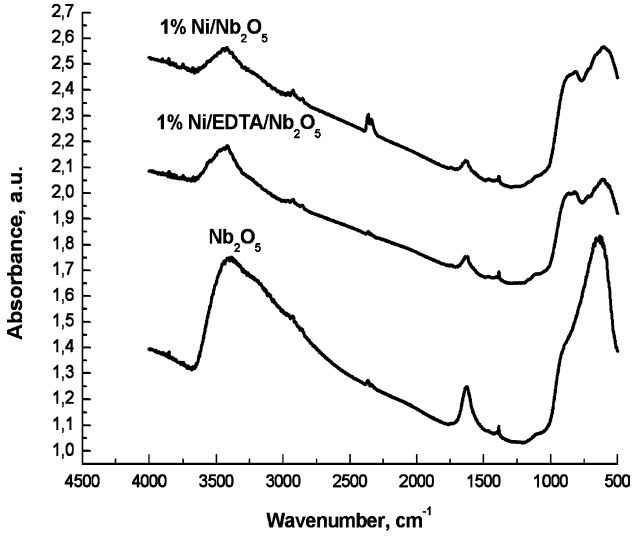

Fig. 2. IR spectra of isopropanol adsorption on the niobium-supported catalysts.

3.2. H_2-TPR profiles

In the TPR conditions used, the SiO_2 and Al_2O_3 supports did not consume hydrogen. In contrast, the control TPR experiments with blank Nb_2O_5 support showed that, when the oxide alone was heated in hydrogen, it started to turn blue at 663 K and was reduced, in good agreement with the literature data [69,72].

3.2.1. Classical catalysts

The H_2-TPR profile of 1% Ni/SiO_2 (Fig. 3) exhibits a broad peak at 892 K with shoulders at around 600 and 1050 K as a result of the formation of several nickel species. The profile of the 1% $Ni/EDTA/SiO_2$ (Fig. 3) catalyst differs from

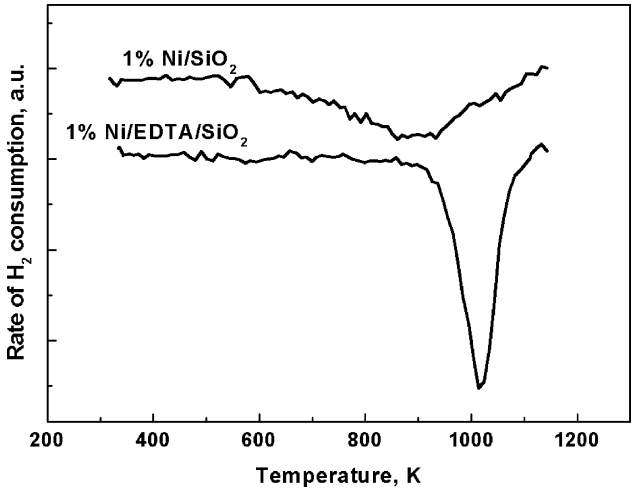

Fig. 3. TPR profiles of classical Ni/SiO_2 catalysts.

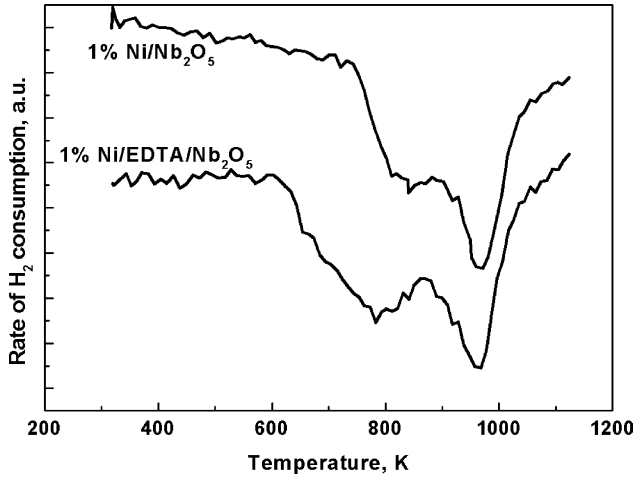

Fig. 4. TPR profiles of classical Ni/Nb_2O_5 catalysts.

that of 1% Ni/SiO_2 one. There is only one sharp peak with the maximum at 1013 K. This lets us to suppose that the catalysts containing EDTA have a better nickel dispersion and the nickel active phase is more homogeneous but it is more difficult to reduce. The high temperature reduction peak comes from the reduction of the nickel cationic form.

Alumina-supported catalysts are not reduced in TPR. It can be caused by strong interaction between the Ni^{2+} ions and the support. The reducibility of Ni-species depends on the nickel–support interaction, which seems to be very high when Al_2O_3 is used as the matrix [19]. The more intense the interaction, the stronger is the connection of Ni-oxide with the matrix. This leads to more difficult interaction with hydrogen. At a low nickel loading, a great number of nickel atoms are in close contact with the support so they are more difficult reduced. At the concentration of the H_2 in the gas flow (1000 ppm), these ions cannot be reduced. In contrast, they are reduced in pure hydrogen at 773 K.

The H_2-TPR profile of the classical niobia-supported catalysts (Fig. 4) shows two broad peaks, with the maximum centered around 800 and 960 K, which originates from the reduction of the different nickel species strongly interacting with the support [72]. Reduction of nickel species depends on the nature of the support. The very strong Ni–niobium oxide interactions are very well known [68–72]. Catalysts, prepared by SIM and DIM, showed nearly the same profiles of the reduction peaks (Fig. 4). However, in case of the 1% $Ni/EDTA/Nb_2O_5$ catalyst, the broad peak starts to appear at a lower temperature. Moreover, the quantity of hydrogen consumed confirmed the higher degree of reduction found for this catalyst.

3.2.2. Non-classical catalysts

The reduction of the supported nickel phase did not occur according to Eq. (1) when the precursors were treated in aqueous hydrazine media at 353 K: the solids became blue and this color was not changed to dark and no nitrogen was detected in the exhaust gas. This may be ascribed to the formation of stable nickel-hydrazine surface species. Indeed, it is known that unsupported Ni^{2+} ions form a blue complex $[Ni(N_2H_4)_3]^{2+}$ in basic hydrazine media [27,73]. This complex is formed via the substitution of water ligands by hydrazine ligands. When the temperature is increased, the complex decomposes and the reaction media progressively changes to a dark black colloidal solution of metallic nickel and gaseous N_2 evolves according to Eq. (1). Moreover, for silica-supported Ni^{2+} ions, it was shown that the reduction occurs in the same hydrazine media with a rate and conversion depending on the nickel content and reaction conditions [27]. It is believed that a supported $[Ni(N_2H_4)_n]^{2+}$ complex, more or less stable, is intermediately formed. It could more or less rapidly decompose to metallic nickel and gaseous N_2.

The non-classical catalysts exhibited typical H_2-TPR profiles. The peaks observed correspond to the reduction of supported Ni^{2+} ions by the hydrogen since aqueous hydrazine reduction was inefficient, as mentioned above. The reducibility of these species depended on the nature of the support and method of preparation and was different from that of Ni^{2+} ions stemming from classical catalysts. In addition, all the non-classical catalysts, strikingly, produced nitrogen around 450 K and hydrogen at higher temperatures. These gases are ascribed to the decomposition of surface NH species previously formed during the hydrazine aqueous treatment. During the TPR experiments, under heating in the gas phase, it decomposed at a higher temperature on the catalyst surface.

A detailed examination of the TPR profiles shows that the temperature of hydrazine decomposition changes with the nature of the support and method of preparation (Table 1). The amount of nitrogen evolving also changed with the nature of the catalyst and, moreover, were larger than that of nickel loading (Table 1). This strongly indicates that hydrazine largely adsorbed on the support in the aqueous media at 353 K, in a way which depended on the nature of the support, in very good agreement with the support acidity reported above. The presence of niobia and EDTA complex gave rise to the largest amounts of hydrazine adsorption and highest N_2 desorption temperature. The results obtained are described below in more details.

The 1% Ni/SiO_2(HYDZ) exhibits a broad H_2-TPR peak (Fig. 5) at a higher temperature (1024 K) than that of the 1% Ni/SiO_2 classical catalyst (1013 K) (Fig. 3). This may

Table 1
N_2 desorption during H_2-TPR studies

Catalyst	Temperature of N_2 desorption (K)	N_2 desorbed $\times 10^{-3}$ (mol g_{cat}^{-1})
1% Ni/Al_2O_3(HYDZ)	458	2.0
1% $Ni/EDTA/Al_2O_3$(HYDZ)	453	8.6
1% Ni/SiO_2(HYDZ)	439	2.2
1% $Ni/EDTA/SiO_2$(HYDZ)	456	2.0
1% Ni/Nb_2O_5(HYDZ)	428, 830	1.1, 0.4
1% $Ni/EDTA/Nb_2O_5$(HYDZ)	480, 838	15.1, 1.1

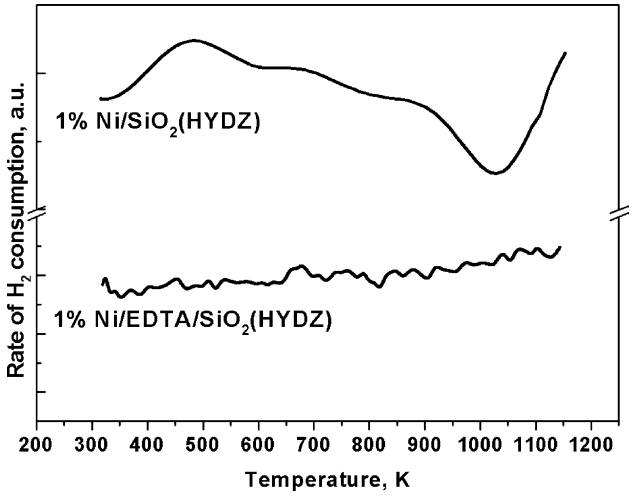

Fig. 5. TPR profiles of non-classical Ni/SiO_2 catalysts.

be due to a stronger interaction with the support which, in turn, probably results from the formation of smaller particles. In contrast, the double impregnation catalyst 1% $Ni/EDTA/SiO_2$(HYDZ) is not reduced at the same conditions (Fig. 5). This confirms desorption of the active phase from the surface of the catalyst during the preparation in hydrazine media (see Section 2). The desorption can be caused by a low stability of Ni/EDTA complex in high pH conditions. Evolution of nitrogen was observed with both silica SIM and DIM non-classical catalysts (Fig. 6A). For these catalysts, the evolution of nitrogen means that the adsorbed hydrazine species decomposition occurs at 450 K. The H atoms of hydrazine probably desorbed as gaseous ammonia which was not analyzed during the TPR measurements. Gaseous hydrazine could decompose as mixtures of nitrogen + ammonia or nitrogen + hydrogen [74,75].

In TPR experiments of non-classical alumina-supported catalysts treated by hydrazine, no hydrogen consumption was observed as a result of a very strong anchorage of the nickel ions on the support. In contrast, a hydrogen production was observed besides that of nitrogen (Fig. 6B). Two types of hydrogen species are observed. The first one appears at around 450 K, concomitantly with nitrogen desorption and the second one at higher temperatures. The peaks at 450 K are ascribed to the partial decomposition of adsorbed hydrazine as nitrogen and hydrogen [74,75]. As to the high temperature peak of hydrogen, it could be due to the formation and incorporation of H-species in the catalyst at 450 K, then desorption at higher temperatures.

The TPR profiles of the niobium-supported catalysts prepared with hydrazine (Fig. 7) differ from those of classical catalysts (Fig. 4). There is only one well-defined peak with maximum at 780–790 K which originates from the reduction of nickel species. Similar TPR profiles were reported for niobia-supported catalysts with larger nickel content (2–15%) [72]. However, the nickel–niobia interaction seems

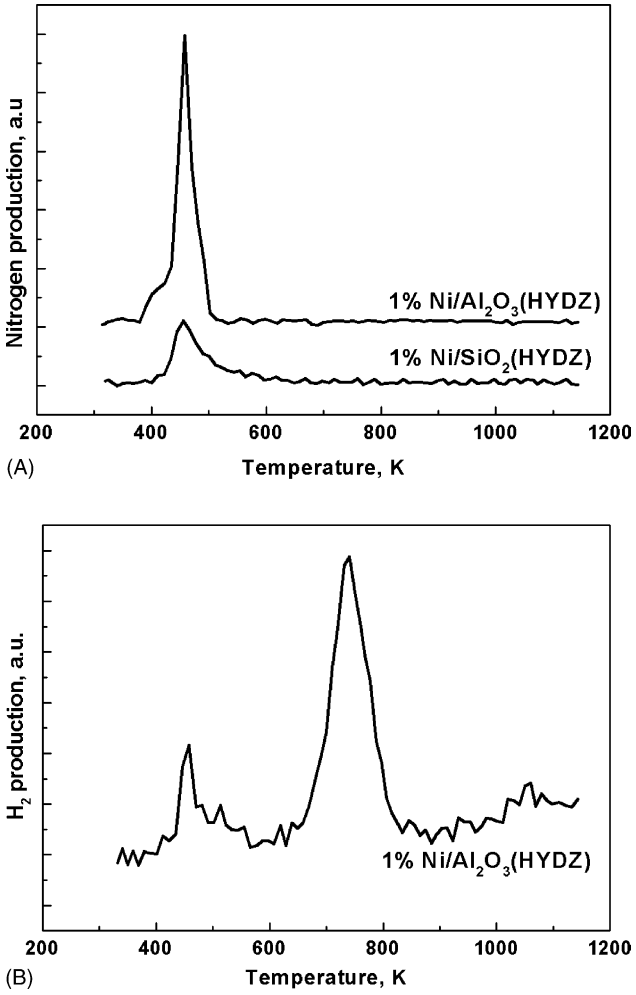

Fig. 6. N_2 production during the TPR for Ni/Al_2O_3(HYDZ) and Ni/SiO_2(HYDZ) catalysts (A) and H_2 production for 1% Ni/Al_2O_3(HYDZ) catalyst (B).

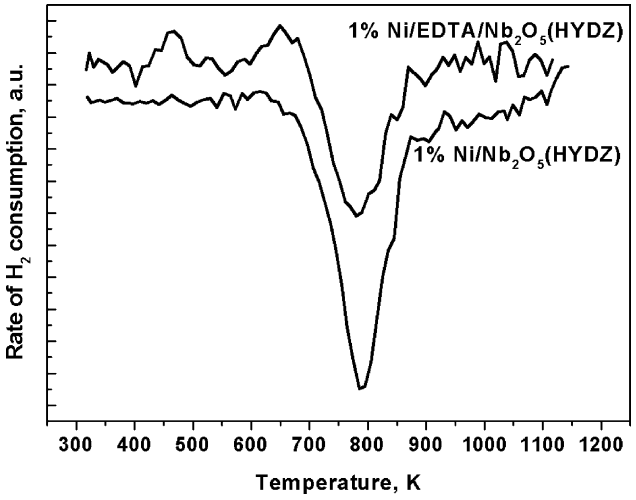

Fig. 7. TPR profiles of non-classical Ni/Nb_2O_5(HYDZ) catalysts.

to be weaker than in case of classical catalysts (Fig. 4). The N_2 desorption, due to the decomposition of hydrazine ions adsorbed on the surface, was also observed.

3.3. Degree of reduction

The degree of reduction was determined after a treatment under pure hydrogen for 2 h at 673 K and 773 K for non-classical and classical catalysts, respectively. In these conditions, all the catalysts were reduced. The amount of reduced nickel atoms was measured by oxygen adsorption at 723 and 823 K for non-classical and classical catalysts, respectively. The obtained results show that the method of preparation or nature of the support determined the degree of reduction. These results are reported in Tables 2 and 3.

The 1% Ni/Al_2O_3 catalyst showed the total reduction (103%), whereas the catalyst prepared by double impregnation was only 86.1% reduced. It can be concluded that double impregnation with H_2Na_2EDTA does not facilitate the reduction of the Ni/Al_2O_3 system. The Al_2O_3 catalysts prepared by the hydrazine reduction exhibited lower degree of reduction, in good agreement with the TPR study which showed that they were of lower reducibility. In the hydrazine treated catalysts, the supported nickel acetate precursor was directly reduced under the hydrogen flow, whereas the classical precursor was previously calcined. Earlier studies have shown that, in some cases, a more complete reduction to metallic nickel could be achieved when the supported nickel salt was directly reduced with hydrogen than when a reduction followed previous calcinations in air [66]. This is not the case here; also, as suggested above, this may be a result of a stronger interaction of nickel with the support for the HYDZ catalysts.

The degree of reduction was found higher for the catalysts supported on Al_2O_3 than that on SiO_2. On SiO_2, the catalyst prepared with H_2Na_2EDTA presented a very low degree of reduction (27%), whereas the catalyst 1% Ni/SiO_2 prepared by simple impregnation showed degree of reduction more than two times higher (68.7%). It could be explained by the TPR study. The TPR profile of this catalyst shows one high temperature reduction peak (Fig. 3). It originates from the reduction of nickel in cationic form. The temperature of the reduction used in this study was not high enough to provide the higher reduction of this catalyst. The SIM catalyst prepared by the chemical treatment with hydrazine showed a higher degree of reduction than the classical one. This is in contrast with the alumina catalysts as a result of the support effect.

It is known that the high temperature reduction of Nb_2O_5 with hydrogen gives the bluish-black dioxide NbO_2 that has a distorted rutile structure [69,76]. This reduction is reversible so the NbO_2 reoxidized gives the Nb_2O_5. Taking into account this reaction, the degree of reduction after H_2 treatment at 773 K was 54.4% for calcined Nb_2O_5. This reaction was also taken into account for calculation of the degree of reduction of the nickel-niobia catalysts.

The classical 1% $Ni/EDTA/Nb_2O_5$ catalysts showed a higher degree of reduction than that of the SIM catalyst (89.3% against 78.2%). One can suppose that EDTA ions could facilitate the reduction of nickel species formed on the surface when Nb_2O_5 support is applied. For Nb_2O_5 support, compared to the classical catalysts, the non-classical cata-

Table 2
Characteristics of the classical catalysts

Catalyst	H_2-adsorption $\times 10^{-3}$ (mol g^{-}_{Ni})	Dispersion (%)	Particle size[a] (nm)	Degree of reduction (%)	TOF (molec Bz h^{-1} $site^{-1}$)	
					373 K	398 K
1% Ni/Al_2O_3	0.35	4.1	24.7	103	6.86	11.71
1% $Ni/EDTA/Al_2O_3$	0.44	5.2	19.5	86.1	10.07	26.84
1% Ni/SiO_2	0.86	10.2	9.9	68.7	37.15	72.11
1% $Ni/EDTA/SiO_2$	0.44	5.0	20.0	27.0	14.24	46.75
1% Ni/Nb_2O_5	0.00	–	–	78.2	0	0
1% $Ni/EDTA/Nb_2O_5$	0.00	–	–	89.3	0	0

[a] From H_2-adsorption.

Table 3
Characteristics of the non-classical catalysts

Catalyst	H_2-adsorption $\times 10^{-3}$ (mol g^{-}_{Ni})	Dispersion (%)	Particle size[a] (nm)	Degree of reduction (%)	TOF (molec Bz h^{-1} $site^{-1}$)	
					373 K	398 K
1% Ni/Al_2O_3(HYDZ)	0.79	9.5	10.6	42.7	2.99	4.06
1% $Ni/EDTA/Al_2O_3$(HYDZ)	0.24	3.0	33.7	70.6	19.48	29.99
1% Ni/SiO_2(HYDZ)	0.71	8.4	12.0	84.6	22.10	46.73
1% $Ni/EDTA/SiO_2$(HYDZ)	0.00	0.0	–	–	0	0
1% Ni/Nb_2O_5(HYDZ)	0.00	–	–	86.6	0	0
1% $Ni/EDTA/Nb_2O_5$(HYDZ)	0.00	–	–	104	0	0

[a] From H_2-adsorption.

lysts showed higher degree of reduction reaching 100% for the 1% Ni/EDTA/Nb_2O_5(HYDZ) material.

3.4. H_2-adsorption study

The H_2-adsorption was used for the determination of the dispersion and particle size of the metal active phase after a pretreatment under a hydrogen flow at 673 or 773 K for the non-classical or classical catalysts, respectively. The results obtained are reported in Tables 2 and 3.

SiO_2, Al_2O_3 and Nb_2O_5 as well as EDTA/SiO_2, EDTA/Al_2O_3 and EDTA/Nb_2O_5 supports did not adsorb hydrogen after the hydrogen thermal pretreatment.

For the classical catalysts, the higher dispersion and smaller nickel particle sizes were found in case of the SiO_2 catalysts. Moreover, the dispersion of the 1% Ni/SiO_2 catalyst is two times higher than that of 1% Ni/EDTA/SiO_2 catalyst. Contrary to that, the dispersion of the double impregnated 1% Ni/EDTA/Al_2O_3 catalyst is higher than that of the SIM catalyst. It could be concluded that introduction of EDTA allows reaching a better dispersion for the catalysts supported on Al_2O_3 while for the silica-supported catalysts EDTA provides growth of the nickel particles. Moreover, the EDTA addition seems to incorporate the nickel ions at the cationic position into the pores of the catalyst while simple impregnation allows creating the surface nickel species. The very high temperature reduction peak (1013 K) observed for this catalyst is similar to the TPR profiles showed in the literature for the catalysts prepared by ion exchange method [77].

Non-classical 1% Ni/EDTA/SiO_2 catalyst did not adsorb the hydrogen at all, which again confirms desorption of the Ni–EDTA complex during the reduction by hydrazine. The more significant part of active phase was out of the catalyst providing absence of the activity for this catalyst. Generally, the classical catalysts prepared by DIM adsorbed more hydrogen than the double impregnated catalysts prepared by the hydrazine reduction. The classical and non-classical catalysts without EDTA adsorb nearly the same quantities of hydrogen.

The SIM as well as DIM prepared catalysts supported on Nb_2O_5 did not adsorb hydrogen. It could be attributed to a very strong interaction of nickel particles with the matrix [69,72]. As suggested from the IR spectra, the nickel ions react with the niobium oxide providing the blockage of the hydrogen adsorption capacity of the nickel. The same results were obtained for the niobium-supported catalysts prepared with the hydrazine. Hydrogen adsorption on Nb_2O_5-supported nickel catalysts has been reported with higher nickel contents (2–15%) [72]. Very low surface areas were found when the reduction temperature was 673 K ($\leq 1\ m^2\ g^{-1}$), i.e. nickel atoms were not very accessible to hydrogen with the niobia support.

3.5. Catalytic activity

After a H_2 thermal treatment, the catalysts became active and selective in the gas phase hydrogenation of benzene to cyclohexane, except of niobia catalysts. No activity was observed without this treatment. The bare silica, alumina or hydrated niobium supports, previously treated or not in aqueous hydrazine, were inactive. The results are reported in Figs. 8 and 9.

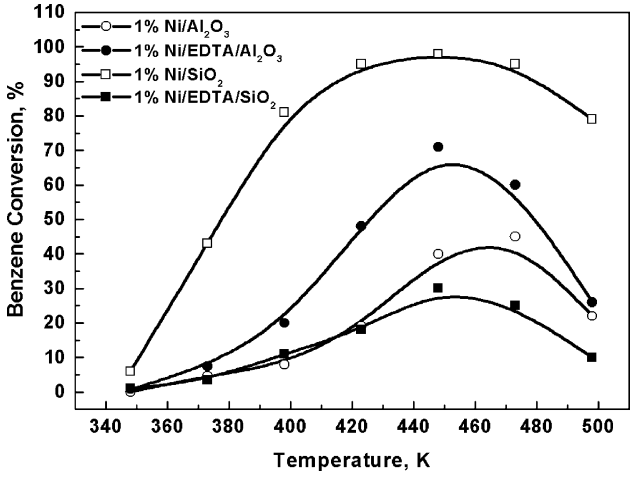

Fig. 8. Conversion of benzene for classical catalysts supported on alumina and silica.

The catalysts exhibited a maximum of activity as a function of the reaction temperature. The temperature of this maximum depends on the method of preparation and nature of the support. It is attributed to the competitive adsorption of the benzene and H_2 reactant molecules [26,57,58]. The activity of the catalysts in the benzene hydrogenation strongly depends on the particle size. It was found that the hydrogenation of benzene reaction is a structure sensitive one [18–20]. In the case of highly dispersed materials, the changes in the catalytic activity were related to the combined effects of particle size, surface coverage with adsorbed species and active site dimension [21].

The best catalytic performances are obtained with the 1% Ni/SiO_2 catalyst which is active from 348 K (6% of con-

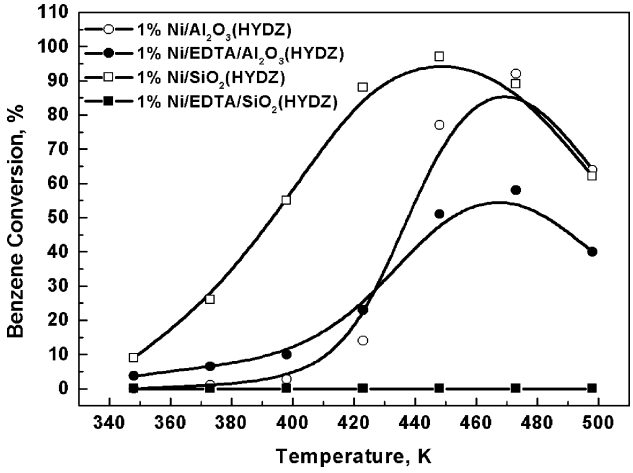

Fig. 9. Conversion of benzene for non-classical catalysts supported on alumina and silica.

version) and totally converts benzene at 448 K (Fig. 8). The double impregnation method leads to a dramatic decrease of the activity: the maximum of conversion hardly reaches 30% for 1% Ni/SiO_2EDTA. For the catalysts supported on SiO_2, the activity increases with increasing the dispersion and decreasing the particle size of the nickel. It could be explained by the reducibility of this catalyst. The maximum of the reduction peaks are 892 and 1013 K (Fig. 3) and the degrees of reduction 27 and 68%, respectively (Table 2). The nickel present on the surface is less reduced and the nickel oxide is not an active phase.

The alumina support decreases the maximum of conversion to 45% and at a higher temperature (473 K) (Fig. 8) as compared to the silica support. In contrast, the double impregnation method enhances the activity since the maximum of conversion increases to 71%, whereas the temperature of this maximum shifts to 175 °C. The lower activity of the alumina catalysts, as compared to that of the silica ones, is due to their lower reducibility as showed from the TPR results (see above). In case of the catalysts supported on alumina, the higher degree of reduction was found for the catalyst prepared by double impregnation (Table 2). Its activity is also higher than that of the catalyst prepared by simple impregnation.

The non-classical 1% Ni/SiO_2 catalyst exhibits similar activity as classical one for the simple impregnation method (Fig. 9). In contrast, the non-classical double impregnation catalyst is completely inactive in benzene hydrogenation. It confirms the desorption of the Ni–EDTA complex when hydrazine was introduced in the liquid media. The more significant part of active phase was out of catalyst, providing the absence of the activity for this catalyst.

When alumina is the support, the non-classical catalyst is more active than the classical one for simple impregnation method: the maximum of conversion passed from 45 to 92% at 474 K (Figs. 8 and 9). In contrast, the double impregnation decreases the maximum conversion from 71 to 58% and increases the temperature of this maximum from 344 to 474 K. Comparison of the non-classical catalysts shows that the double impregnation decreases the maximum conversion from 71 to 51% at 448 K.

The results of the benzene hydrogenation could be well correlated with the dispersion of nickel active phase. For the non-classical catalysts supported on Al_2O_3, the activity increases with increasing the dispersion and decreasing the particle size of nickel. The 1% Ni/SiO_2 and 1% Ni/Al_2O_3 non-classical catalysts have a dispersion and catalytic activity comparable at high reaction temperatures. At lower reaction temperatures, the former is much more active due to a better reducibility as showed from the TPR and degree of reduction experiments.

In contrast to the SiO_2 and Al_2O_3 catalysts, the niobia-supported catalysts, classical or non-classical, are not active in the hydrogenation of benzene to cyclohexane. The absence of activity is ascribed to very strong metal–support interactions, which make the adsorption of the reactant molecules on nickel not enough sufficient for the further hydrogenation process.

4. Conclusions

The surface acidity of the supports used changes as manifested by the isopropanol test-reaction: $SiO_2 < Al_2O_3 < Nb_2O_5$. The incorporation of Ni^{2+} ions in the oxide matrix by simple or double impregnation method gives rise to metal–support interactions which are the strongest for the niobia support as showed by the IR study.

Various nickel surface species were evidenced by the H_2-TPR study. According to the method used or/and support, the nickel phase exhibited various reducibility, surface or hydrogenating properties, after calcinations, then reduction under a hydrogen atmosphere. These properties also changed when the supported precursors were treated in aqueous hydrazine, then directly reduced in hydrogen atmosphere. As a general trend, the best performances are obtained with the silica support, which seems to interact less with the nickel. The metal–support interactions are highest when niobium oxide is used as the matrix for nickel. Also, Ni supported on hydrated niobia was not active towards hydrogen or hydrogen + benzene systems.

The supported precursors were shown to be not reduced in aqueous hydrazine at 353 K, as initially desired, because a stable blue surface complex $[Ni(N_2H_4)_n]^{2+}$ was formed. In the mean time, hydrazine molecules adsorbed on the catalyst support in the aqueous media. These molecules decomposed to gaseous mixtures N_2 (+NH_3) or $N_2 + H_2$ according to the nature of the support with amounts and at a temperature depending on the support acidity, in good agreement with the isopropanol test-reaction and IR studies.

References

[1] S.J. Tautster, S.C. Fung, J. Catal. 5 (1978) 29.
[2] C.H. Bartholomew, Mustard, J. Catal. 67 (1981) 186.
[3] W.P. Halperin, Rev. Mod. Phys. 58 (1998) 533.
[4] G. Schmid, Chem. Rev. 92 (1992) 1709.
[5] J.S. Bradley, E.W. Will, C. Klein, B. Chaudret, A. Duteil, Chem. Mater. 5 (1993) 2540.
[6] H. Hirai, Y. Nakao, N. Toshima, J. Macromol. Sci. Chem. A 13 (1979) 727.
[7] L.N. Lewis, Chem. Rev. 93 (1993) 2693.
[8] Y. Volotkin, J. Sinzig, L.J. De Jong, G. Schmid, M.N. Vargaftik, I.I. Moisseev, Nature 384 (1996) 621.
[9] V.N. Colvin, M.C. Schlamp, A.P. Alivisatos, Nature 370 (1994) 354.
[10] R.L. Whetten, Acc. Chem. Res. 32 (1999) 397.
[11] J. Ryczkowski, T. Borowiecki, React. Kinet. Catal. Lett. 49 (1) (1993) 127.
[12] J. Ryczkowski, T. Borowiecki, D. Nazimek, Adsorp. Sci. Technol. 14 (2) (1996) 113.
[13] B.C. Gates, Chem. Rev. 95 (1995) 511.
[14] R. Brayner, G. Viau, F. Bozon-Verduraz, J. Mol. Catal. A 182/183 (2002) 227.
[15] W. Yu, H. Liu, X. Ma, Z. Liu, J. Colloid Interface Sci. 208 (1998) 439.

[16] T.S. Armadi, Z.L. Wang, T.C. Green, A. Heinglein, M.A. El-Sayed, Science 272 (1996) 24.
[17] J. Zelinski, J. Catal. 76 (1982) 157.
[18] J.T. Richardson, M. Lei, B. Turk, K. Forster, M.V. Twigg, Appl. Catal. 110 (1994) 217.
[19] R. Molina, G. Poncelet, J. Catal. 173 (1998) 257.
[20] A. Miyazaki, I. Balin, K. Aika, Y. Nakano, J. Catal. 204 (2001) 364.
[21] D. Reinen, P.W. Selwood, J. Catal. 2 (1963) 109.
[22] M. Houalla, J. Lemaître, B. Delmon, J. Chem. Soc. Faraday Trans. 78 (1982) 1389.
[23] W. Schwieger, O. Gravenhorst, T. Selva, F. Roessner, R. Schloegl, D. Su, G.T.P. Mabande, Colloid Polym. Sci. 281 (2003) 584.
[24] U.A. Paulus, U. Endrushchat, G.J. Feldmeyer, T.J. Schmidt, H. Bonnemann, R.J. Behm, J. Catal. 195 (2000) 383.
[25] E.A. Sales, B. Benhamida, V. Caizergues, J.P. Lagier, F. Fievet, F. Bozon-Verduraz, Appl. Catal. 172 (1998) 273.
[26] A. Boudjahem, S. Monteverdi, M. Mercy, M.M. Bettahar, J. Catal. 221 (2004) 325.
[27] A. Boudjahem, S. Monteverdi, M. Mercy, M.M. Bettahar, Langmuir 20 (2004) 208.
[28] L.K. Kurihara, G.M. Chow, P.E. Shoen, Nanostruct. Mater. 5 (1995) 607.
[29] T.D. Xiao, S. Torban, P.R. Strut, B.H. Kear, Nanostruct. Mater. 7 (1996) 857.
[30] J.H. Fendler, F.C. Meldrum, Adv. Mater. 7 (1995) 607.
[31] F. Fievet, F. Fievet-Vincent, J.P. Lagier, B. Dumont, M. Figlarz, J. Mater. Chem. 3 (1993) 627.
[32] R.D. Rieke, Acc. Chem. Res. 10 (1997) 377.
[33] R.D. Rieke, Science 246 (1989) 1260.
[34] G.A. Ozin, Adv. Mater. 4 (1992) 612.
[35] G.N. Glavee, Inorg. Chem. 32 (1993) 474.
[36] H. Bonnemain, W. Brijoux, T. Joussen, Angew. Chem. Int. Ed. Engl. 29 (1990) 273.
[37] D. Zeng, M.J. Hampten-Smith, Chem. Mater. 5 (1993) 68.
[38] K. Vijaya Sarathy, G.U. Kulkarny, C.N.R. Rao, Chem. Commun. (1997) 537.
[39] P. Gallezot, C. Leclercq, Y. Fort, P. Caubere, J. Mol. Catal. 93 (1994) 79.
[40] J.J. Brunet, P. Gallois, P. Caubere, J. Org. Chem. 45 (1980) 1937.
[41] N. Toshima, Y. Wang, Adv. Mater. 6 (1994) 245.
[42] A. Heinglein, J. Phys. Chem. 97 (1993) 5457.
[43] J.S. Bradley, J.M. Millar, E.W. Hill, S. Behal, B. Chaudret, Faraday Discuss. 92 (1991) 255.
[44] J.C. Poulin, H.B. Kagan, M.N. Vargavtik, I.P. Stolarov, I.I. Moisseev, J. Mol. Catal. 95 (1995) 109.
[45] T. Mostafa, A.M. Cordonnier, C. Santini, J.M. Basset, J.P. Candy, New J. Chem. 28 (2004) 1531.
[46] N. Toshima, T. Takahashi, Bull. Chem. Soc. Jpn. 65 (1992) 400.
[47] K. Esumi, K. Matzuhita, K. Torigoe, Langmuir 11 (1995) 3285.
[48] D.V. Leff, P.C. Ohara, J.R. Heath, W.M. Gelbart, J. Phys. Chem. 99 (1995) 7036.
[49] H. Bönnemann, W. Brijoux, R. Brinkmann, E. Dinjus, E. Joussen, B. Korall, Angew. Chem. Int. Ed. Engl. 30 (1991) 1312.
[50] M.T. Reetz, W. Helbig, J. Am. Chem. Soc. 116 (1994) 7401.
[51] N. Toshima, T. Teranishi, H. Asanuma, Y. Saito, J. Phys. Chem. 96 (1992) 3796.
[52] S.J. Tauster, Acc. Chem. Res. 20 (1987) 389.
[53] R. Brayner, G. Viau, G.M. da Cruz, F. Fiévet-Vincent, F. Fiévet, F. Bozon-Verduraz, Catal. Today 57 (2000) 187.
[54] J.L. Pellegatta, C. Blandy, V. Collière, R. Choukroun, B. Chaudret, P. Cheng, K. Phillipot, J. Mol. Catal. A 178 (2002) 55.
[55] A. Stanislaus, B.H. Cooper, Catal. Rev. Sci. Eng. 36 (1994) 75.
[56] K. Weissermel, H.J. Arple, Industrial Organic Chemistry, third ed., VCH, New York, 1997.
[57] M.A. Keane, J. Catal. 166 (1997) 347.
[58] R. Molina, G. Poncelet, J. Catal. 199 (2001) 162.
[59] B. Coughlan, M.A. Keane, Zeolites 11 (1991) 12.
[60] K.J. Yoon, M.A. Vannice, J. Catal. 82 (1983) 457.
[61] L. Daza, B. Pawelec, J.A. Anderson, J.L.G. Fierro, Appl. Catal. 87 (1992) 145.
[62] R. Burch, R. Flambard, J. Catal. 85 (1984) 16.
[63] A. Bensalem, G. Shafeev, F. Bozon-Verduraz, Catal. Lett. 18 (1993) 165.
[64] Y.D. Li, L.Q. Li, H.W. Liao, H.R. Wang, J. Mater. Chem. 9 (1999) 2675.
[65] L.M. Bronstein, O.A. Platonova, A.N. Yakunin, I.M. Yanovskaya, P.M. Valetsky, A.T. Dembo, E.S. Obolonkova, E.E. Makhaeva, A.V. Mironov, A.R. Khokhlov, Colloid Surf. 147 (1999) 221.
[66] C.H. Bartholomew, R.J. Farrauto, J. Catal. 45 (1976) 41.
[67] G. Bergeret, P. Gallezot, in: G. Erlt, H. Knozinger, J. Weitkamp (Eds.), Handbook of Heterogeneous Catalysis, vol. 2, VCH, Weinheim, 1997, p. 439.
[68] A. Lewandowska, S. Monteverdi, M. Bettahar, M. Ziolek, J. Mol. Catal. A: Chem. 3713 (2002) 1.
[69] E.I. Ko, J.M. Hupp, F.H. Rogan, N.J. Wagner, J. Catal. 84 (1983) 85.
[70] E.I. Ko, J.M. Hupp, N.J. Wagner, J. Catal. 86 (1984) 315.
[71] T. Fung, J. Am. Chem. Soc. 100 (1978) 170.
[72] K.V.R. Chary, K.S. Lakshmi, P.V. Ramana Rao, K.S. Rama Rao, M. Papadaki, J. Mol. Catal. A: Chem. 223 (2004) 353.
[73] Y.D. Li, L.Q. Li, H.W. Liao, H.R. Wang, J. Mater. Chem. 9 (1999) 2675.
[74] X. Chen, T. Zhang, M. Zheng, Z. Wu, W. Wu, C. Li, J. Catal. 224 (2004) 473.
[75] R. Brayner, G. Djéga-Mariadassou, G. Marques da Cruz, J.A.J. Rodrigues, Catal. Today 57 (2000) 225.
[76] I. Nowak, M. Ziolek, Chem. Rev. 99 (1999) 3603.
[77] R. Wojcieszak, S. Monteverdi, M. Mercy, I. Nowak, M. Ziolek, M.M. Bettahar, Appl. Catal. A: Gen. 268 (2004) 241.